



OPEN

# Generation of a functional liver tissue mimic using adipose stromal vascular fraction cell-derived vasculatures

S. S. Nunes<sup>†</sup>, J. G. Maijoub, L. Krishnan<sup>‡</sup>, V. M. Ramakrishnan, L. R. Clayton, S. K. Williams, J. B. Hoying\* & N. L. Boyd\*

Cardiovascular Innovation Institute, University of Louisville, Louisville, KY, USA.

SUBJECT AREAS:

ANGIOGENESIS

TISSUE ENGINEERING

CELL BIOLOGY

CELL DELIVERY

Received  
17 April 2013

Accepted  
19 June 2013

Published  
5 July 2013

Correspondence and requests for materials should be addressed to

J.B.H. (jay.hoying@louisville.edu) or N.L.B. (nolan.boyd@louisville.edu)

\* These authors contributed equally to this work.

<sup>†</sup> Current address: Toronto General Research Institute, University Health Network, Toronto, Canada.

<sup>‡</sup> Current address: Institute for Bioengineering and Bioscience (IBB), Georgia Institute of Technology, Atlanta, GA.

One of the major challenges in cell implantation therapies is to promote integration of the microcirculation between the implanted cells and the host. We used adipose-derived stromal vascular fraction (SVF) cells to vascularize a human liver cell (HepG2) implant. We hypothesized that the SVF cells would form a functional microcirculation via vascular assembly and inosculation with the host vasculature. Initially, we assessed the extent and character of neovasculatures formed by freshly isolated and cultured SVF cells and found that freshly isolated cells have a higher vascularization potential. Generation of a 3D implant containing fresh SVF and HepG2 cells formed a tissue in which HepG2 cells were entwined with a network of microvessels. Implanted HepG2 cells sequestered labeled LDL delivered by systemic intravascular injection only in SVF-vascularized implants demonstrating that SVF cell-derived vasculatures can effectively integrate with host vessels and interface with parenchymal cells to form a functional tissue mimic.

Tissue replacement is a potential strategy for regeneration of different organs affected in multiple conditions such as organ failure and congenital abnormalities. Cell transplantation offers an alternative to treat patients with organ failure, such as in liver diseases<sup>1,2</sup>. However, minimal engraftment is achieved with this approach<sup>1,3,4</sup>. One of the major caveats in tissue replacement therapies is to promote effective vascularization of the transplanted tissue in order to prevent death and promote engraftment of transplanted cells. Several approaches have been utilized in an attempt to promote vascularization of implanted tissues such as the delivery of angiogenic growth factors to recruit host vessels or co-implantation of endothelial and angiogenic signaling cells with target tissue cells (reviewed in<sup>5,6</sup>). Although considerable progress has been achieved, significant obstacles such as short half-life of growth factors in the tissues resulting in regression of newly formed vasculatures<sup>7,8</sup> and potential source of endothelial and angiogenic signaling cells for human transplants still need to be addressed.

Adipose-derived stromal vascular fraction (SVF) cells are an attractive cell population identified for transplantation studies since human adipose tissue is an easily accessible and dispensable tissue source that can provide large numbers of cells suitable for implantation with little donor morbidity and patient discomfort. In addition, SVF cell preparations have been shown to be safely and effectively transplanted to either an autologous or allogeneic host and can be manufactured in accordance with Good Manufacturing/Tissue Practice guidelines<sup>9</sup>.

SVF cells are obtained from the enzymatic digestion of adipose tissue to single cells followed by discarding adipocytes. They are a mix of heterogeneous cell populations composed of endothelial cells, fibroblasts, perivascular cells, immune cells and undefined stem cell sub-populations<sup>10–12</sup>. The potential of SVF cells to promote vascularization and improve organ function when delivered to sites of ischemia has been demonstrated in animal models of peripheral ischemic disease<sup>13–15</sup> and myocardial infarction<sup>16,17</sup>.

Here, our goal was to harness the vascularization potential of SVF cells *in vivo* to generate an effective vascular interface between host and transplanted liver cells resulting in a functional tissue mimic. We show that (1) adipose-derived SVF cells have a potent intrinsic vascularizing potential, (2) culturing freshly isolated SVF cells retains this vascularization potential despite possible changes in cell populations, and (3) SVF cell-derived vasculatures form a functional interface between host and implanted parenchymal cells.

## Results

**Adipose stromal vascular fraction cells form perfused microvasculatures.** One of the key technical hurdles for developing a functional tissue mimic is providing a vascular interface between the host circulation and implanted



parenchymal cells. The freshly isolated stromal vascular fraction (SVF) from adipose is rich in vascular and other relevant cells<sup>18</sup> capable of incorporating into vessels *in vivo*<sup>14</sup>. Similarly, cultured SVF cell populations also exhibit vascularizing potential<sup>19,20</sup>, supporting the use of both fresh and cultured SVF cells (fSVF and cSVF, respectively) as cell sources in transplantation therapies. Based on these past findings, we hypothesized that adipose SVF cells alone are capable of forming *de novo* a new vasculature that would be amenable to use in vascularizing a tissue mimic. To test this hypothesis, we used SVF cell preparations from transgenic rats ubiquitously expressing GFP<sup>21</sup> to form implants. As predicted, both fSVF and cSVF cells in a simple 3D collagen matrix free of exogenous growth factors self-assembled to form a perfused vasculature (Fig. 1). For both SVF cell preparations, complete vascular trees consisting of arterioles, capillaries and venules were observed and comprised entirely of GFP<sup>+</sup> cells, indicating an SVF origin (Fig. 1). While both fSVF and cSVF generated perfused vasculatures, those formed by cSVF had lower vessel densities than fSVF-derived vasculatures (fSVF,  $94.9 \pm 22$ ; cSVF,  $59.2 \pm 8$  vessels/field of view) and total vessel perfusion was significantly less, (fSVF,  $97.4 \pm 0.8$ ; cSVF,  $86.7 \pm 1.9$ ) (Fig. 1). Additionally, the average vessel diameter within the cSVF-formed vasculatures was significantly higher suggesting a lower proportion of smaller capillary-like diameters than in fSVF-formed vasculatures (fSVF,  $11.7 \pm 1.5$ ; cSVF,  $14.6 \pm 2.3$ ) (Fig. 1).

**Adipose stromal vascular fraction cells contribute to angiogenesis.** Another critical issue with functionalizing an implanted tissue mimic is efficient integration between the mimic-host vasculatures. Using an experimental model of neovascularization involving the implantation of angiogenic microvessels<sup>22,23</sup>, we next investigated the ability of SVF cells to incorporate into an angiogenic vascular bed, an activity essential to vascular integration. As with *de novo* vessel assembly, both fresh and cultured SVF cells participated in the formation of new vessel elements during active angiogenesis (Fig. 2). During the early phases of neovascularization, which is dominated by angiogenesis and immature network formation, SVF

cells were intimately associated with the nascent, endothelial cell-derived neovessels throughout the developing neovasculature. In the later implants, the mature vasculatures that formed were comprised of GFP<sup>+</sup> (i.e. SVF-derived) and GFP-negative (i.e. non-SVF-derived) cells (Fig. 2). Moreover, many of the non-SVF-derived vessels were populated with SVF cells or were chimeras of non-SVF-derived and SVF-derived vessel segments (Fig. 2). In mature angiogenic implants containing fSVF, GFP<sup>+</sup> cells were observed in endothelial and perivascular positions of all vessel types. In contrast, cSVF cells were found predominately in perivascular positions and rarely in the endothelial position (Fig. 2). In addition, the extent of cSVF cell incorporation into the formed vasculature was approximately half that of fSVF cells (fSVF,  $24.6 \pm 10.4\%$ ; cSVF,  $13 \pm 6.6\%$ ) (Fig. 2).

**Cultured SVF cells have fewer CD31 and cKit positive cells than fresh SVF cells.** These differences in incorporation potential and vascular position suggest that submitting SVF cells to culture promotes either a selection of a perivascular phenotype or changes in the population potential. To investigate the different cell populations present in fresh and cultured SVF, we assessed the expression of different cell type markers by flow cytometry (Fig. 3). Consistent with the vascularizing potential and predicted from a related study<sup>14</sup>, cSVF cell population contains less than half the number of CD31<sup>+</sup> cells (presumably endothelial cells) than fSVF cells (Fig. 3). Similarly, the proportion of c-Kit<sup>+</sup> progenitor cells was greatly reduced in cSVF cells as compared to fSVF cells. However, the proportions of cells expressing markers for monocyte/macrophages (CD14), perivascular cells (PDGFR- $\beta$ ) and multipotent cells (CXCR4, c-Met) was not different (Fig. 3). The similar presence of PDGFR- $\beta$ <sup>+</sup> cells in both SVF preparations might explain the shared potential for establishing mural/perivascular coverage of the new vessel elements.

**Human freshly isolated adipose SVF cells vascularize implanted parenchymal cells.** Having demonstrated the vascularizing potential of SVF cells using a transgenic lineage marker, we next determined the vascularizing potential of clinically relevant human SVF cells. To do this, we repeated the above *de novo* assembly experiments using

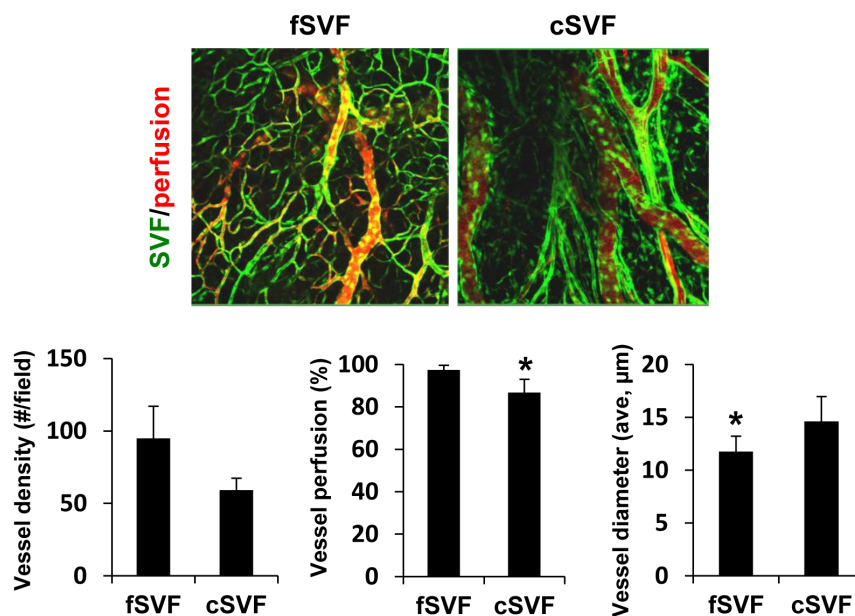


**Figure 1 | Adipose stromal vascular fraction cells form perfused microvasculatures in vivo.** Fresh (fSVF) and cultured (cSVF) isolated from GFP rats were seeded in 3-dimensional collagen type I gels and implanted subcutaneously into immunocompromised mice. After 4 weeks, host mice were perfused with dextran-TRITC through jugular injection. Representative images of vasculatures formed 4 weeks post-implantation are shown. Vessel density (number of vessels/field of view), percentage of vessels perfused (\* $p = 0.001$ ) and average vessel diameter (\* $p = 0.02$ ) are shown. Values are reported as mean  $\pm$  s.e.m.;  $n = 3$ /condition.

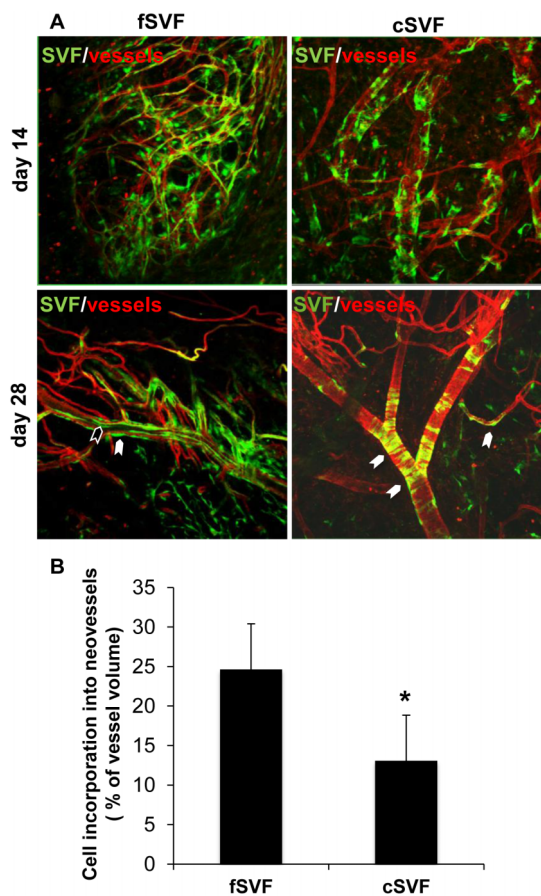


**Figure 2 | Adipose stromal vascular fraction cells contribute to angiogenesis.** Freshly isolated and cultured SVFs significantly differ in their ability to incorporate into sites of neovascularization. fSVF and cSVF isolated from GFP rats were co-implanted with microvessel fragments derived from non-GFP rats into immunocompromised mice for 14 or 28 days, when implants were removed and vessels stained with GSI-TRITC. Representative images of vasculatures formed 14 and 28 days post-implantation. Black arrow shows SVF in endothelial cell position. White arrows show SVF incorporated in perivascular position. Quantification of SVF incorporation into neovessels 28 days post-implantation (percentage of total vessel volume) Values are reported as mean  $\pm$  s.d.; \* $p = 0.01$ ,  $n = 4$  (fSVF);  $n = 8$  (cSVF).

freshly isolated SVF cells derived from discarded lipo-aspirates with the exception that the SVF cells in collagen constructs were implanted for 6 weeks instead of 4 weeks. As with the rat SVF cells, the human SVF cells were also able to self-assemble into a vascular network, although the human SVF-derived network may still be undergoing neovascular remodeling<sup>24</sup> at this time (Fig. 4). To determine if the human SVF cells retained this ability to assemble a vasculature *de novo* in the presence of parenchyma cells, we implanted constructs containing human SVF with HepG2 cells, an hepatocyte-like cell line<sup>25</sup>, grown on Cytodex-3 beads to maintain the hepatocyte-like phenotype in the 3-D environment<sup>26</sup>. As before, the human SVF cells assembled a vascular network in these implants (Fig. 4). Interestingly, human SVF-derived vessel networks formed around and in close approximation to the HepG2 clusters (Fig. 4).

**Freshly isolated adipose SVF cells functionally interface with implanted parenchymal cells.** Because of the close association between SVF cell-derived vessels and HepG2 clusters, we next determined if this vascularized cell system was functional. To do this, we took advantage of the fact that HepG2 cells express the LDL receptor and take up LDL similar to mature hepatocytes<sup>27</sup> by

examining LDL uptake in the vascularized implants. As expected, HepG2 cell implants vascularized with fresh SVF cells took up DiI-labeled LDL (DiI-LDL) injected intravenously into the host mouse (Fig. 5). Approximately 83% of the HepG2 clusters were associated with a vascular network or DiI-LDL uptake, while approximately 67% of the HepG2 clusters were associated with both. Further analysis indicates a strong correlation ( $r = 0.909$ ) between the presence of vessels and DiI-LDL uptake by HepG2 cell clusters (Fig. 5). Indeed, HepG2 clusters not associated with a vasculature did not co-localize with DiI-LDL despite DiI-LDL uptake by host liver (Fig. 5).

## Discussion

With a relatively simple strategy, we show for the first time that functional, vascularized tissue mimics can be generated by combining parenchymal and adipose-derived SVF cells. In this case, the tissue mimic was a model liver module using a human model hepatocyte cell line (HepG2) as the parenchyma. Central to this strategy is the ability of adipose-derived SVF cells (either freshly isolated or cultured) to spontaneously form *de novo* a mature microvasculature. Importantly, the uptake of LDL by the HepG2 cells demonstrates that this formed microvasculature serves as a functional vascular interface between the host circulation and the parenchymal cells. The vascular-parenchyma integration observed in the SVF-based implant, intrinsic to native tissues, highlights the therapeutic potential of this implant design/strategy. While we demonstrated proof-of-principle using a liver tissue mimic, we envision this use of adipose SVF cells as an enabling solution with broad applicability. Related to this and due to the inherent vascularization ability of isolated adipose SVF cells, we envision a point-of-care strategy whereby freshly harvested SVF cells from readily acquired lipoaspirates can be used in an autologous fashion. Conversely, given that cultured SVF cells retain the ability to form *de novo* blood-perfused vasculatures, a more therapeutically convenient “off-the-shelf” approach could be employed by using banked, pooled adipose SVF cells expanded by culture (albeit low passage number). The low immunogenicity of adipose-derived cells<sup>16,28</sup> makes the allogeneic approach feasible. This immune-privileged aspect of adipose SVF cells may even facilitate the use of allogeneic parenchymal cells in the implant design should an autologous solution not be available<sup>29,30</sup>. Finally, multiple Phase I clinical trials using different adipose-derived SVF preparations as a source for therapeutic mesenchymal cells indicate that these cells are very safe<sup>31</sup>.

Previous attempts towards the development of vascularized liver grafts for transplantation consisted of incorporating vascular endothelial growth factor into scaffolds to enhance vascularization of transplanted hepatocytes<sup>32</sup>. However, the authors did not investigate vessel perfusion or function of implanted hepatocytes. Here we demonstrate that when combined with HepG2 parenchymal cells, SVF cell-derived vasculatures envelop these cells, forming a functional interface. Indeed, we demonstrate the effective integration of transplanted liver tissue mimics six weeks post-implantation through the metabolic interaction between SVF formed vessels and parenchyma cells, as illustrated by the uptake of fluorescently labeled LDL by HepG2 cells. This proof-of-principle system suggests that other therapeutic cells could be combined with SVF to form modular tissue mimics for delivery or removal of circulating biomolecules.

The simple liver tissue mimic was developed as a modular system designed to perform a specific function (LDL uptake in this case). Similarly, tissue mimic modules with different functional purposes could be assembled by incorporating different parenchymal cells along with the vascularizing adipose SVF cells. In this way, via our modular approach, more complex organoids capable of performing multiple, potentially integrated, physiological functions could be generated by combining these different multiple tissue mimics. This modular strategy is also scalable by simply implanting more or less of the modules to meet therapeutic need. Additionally, select

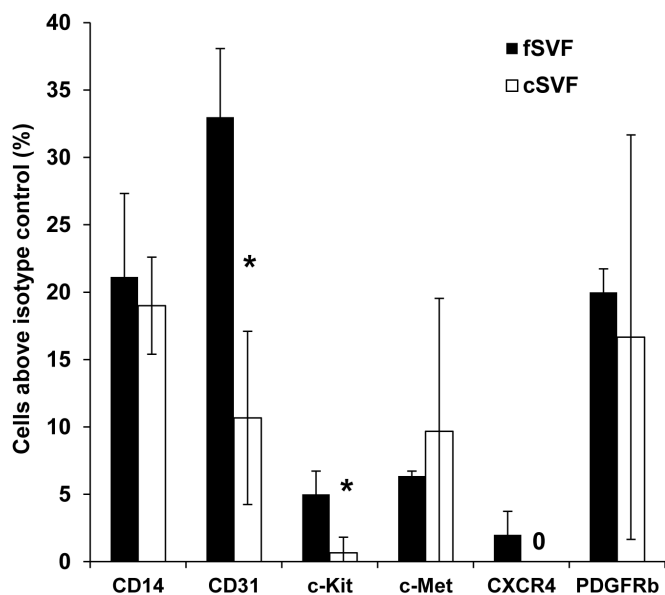


**Figure 3** | Expression of cell surface markers in freshly isolated (black bars) and cultured (white bars) SVF cells. Cells were stained for the different molecules and analyzed by fluorescent flow cytometry. Percentage of cells positive for a specific molecule above isotype control is shown. Values are reported as mean  $\pm$  s.d.; \* $p = 0.009$  (CD31) and  $0.02$  (c-kit);  $n = 3$ /condition. At the 95% confidence level,  $\alpha = 0.929$ .

modules (or all) could be removed should there be an unexpected, deleterious outcome to the implantation (e.g. infection). Depending on the configuration, these mimics, such as the liver mimic presented here, could prove useful not only as an implantable functional replacement (e.g. LDL clearance) for regenerative medicine, but also as a human model tissue system for triaging/developing drug candidates targeting specific parenchyma types, evaluating drug metabolism (as with the hepatocyte-like module), and other translational and mechanistic investigations.

While the inherent vascularization capability of adipose SVF cells is maintained in early passage culture, the capacity of these cells to incorporate into vascular sites of neovascularization (i.e. angiogenic

neovessels) is altered, suggesting that culturing has an effect on the SVF cells. This is demonstrated not only by the significant decrease in SVF incorporation into formed neovessels but also by the position of the incorporated cells (endothelial and perivascular for fresh SVF; mostly perivascular for cultured SVF). Flow cytometry of select markers revealed a significant decrease in the percentage of CD31<sup>+</sup> and cKit<sup>+</sup> cells after culture, suggesting a reduction in the proportion of endothelial cell phenotypes<sup>33–35</sup>. This reduction corresponds to a lower density (i.e. number) of vessels formed *de novo* by the cultured SVF cells and is consistent with the idea that the endothelial cells present in an adipose SVF cell isolate are required for vascular assembly<sup>14</sup>. Interestingly, the proportion of cells with perivascular phenotype (PDGFR- $\beta$ <sup>+</sup> cells)<sup>36,37</sup> did not change with culture. Again, this is consistent with the observation that cultured SVF cells preferentially incorporated into the mural position in angiogenic neovessels.

It's important to note that plating and culture conditions we employed differ from those used by others selecting for adipose-derived stem cells (ADSC)<sup>20,38</sup>. While there are cells expressing mesenchymal stem cell-like markers in our early-passage, cultured SVF cells, we clearly have mixed cell phenotypes present that are not typically observed in the other reported ADSC phenotypes. These mixed phenotypes observed in our cultured SVF cells may explain why the cultured SVF cells are able to generate *de novo* a vasculature (as all necessary cell types appear to be present), albeit to a lesser extent than with the freshly isolated SVF cells. Whether or not extended culturing of the SVF cells (beyond P0 or P1) alters further cell phenotypes and, consequently, the vascularizing ability remains to be determined.

One of the most intriguing aspects of the current study is the ability of SVF cells, either fresh or cultured, to go from a single-cell suspension to a self-assembled functionally mature vasculature. At present it is unknown how this heterogeneous cell mix works together to reassemble back into a vasculature or which specific cell types are necessary. As shown by Koh, et al<sup>14</sup>, and indicated here, endothelial cells play an essential role in this process. However, endothelial cells alone are insufficient to form a mature vasculature either *in vitro*<sup>39</sup> or *in vivo*<sup>40</sup>. Clearly non-endothelial support cells are required to achieve vessel stabilization and maturation<sup>39,41</sup>. Within the SVF are these support cells, such as perivascular cells and/or mesenchymal stem cells. But, also other stromal cells present in the isolate, such as fibroblasts and macrophages, may be important<sup>12,42</sup>.

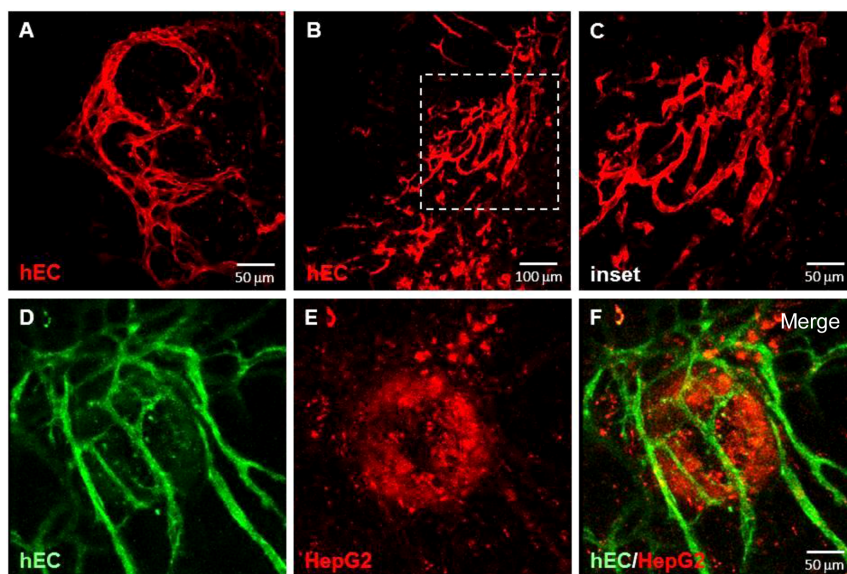


**Figure 4** | Human freshly isolated adipose SVF cells vascularize implanted parenchymal cells. (A–C) Freshly isolated human SVF seeded in collagen type I gels and implanted subcutaneously into immunocompromised mice. After four weeks, implants were stained with UEA-TRITC. (D–F) Human SVF and HepG2 beads constructs implanted for 6 weeks.

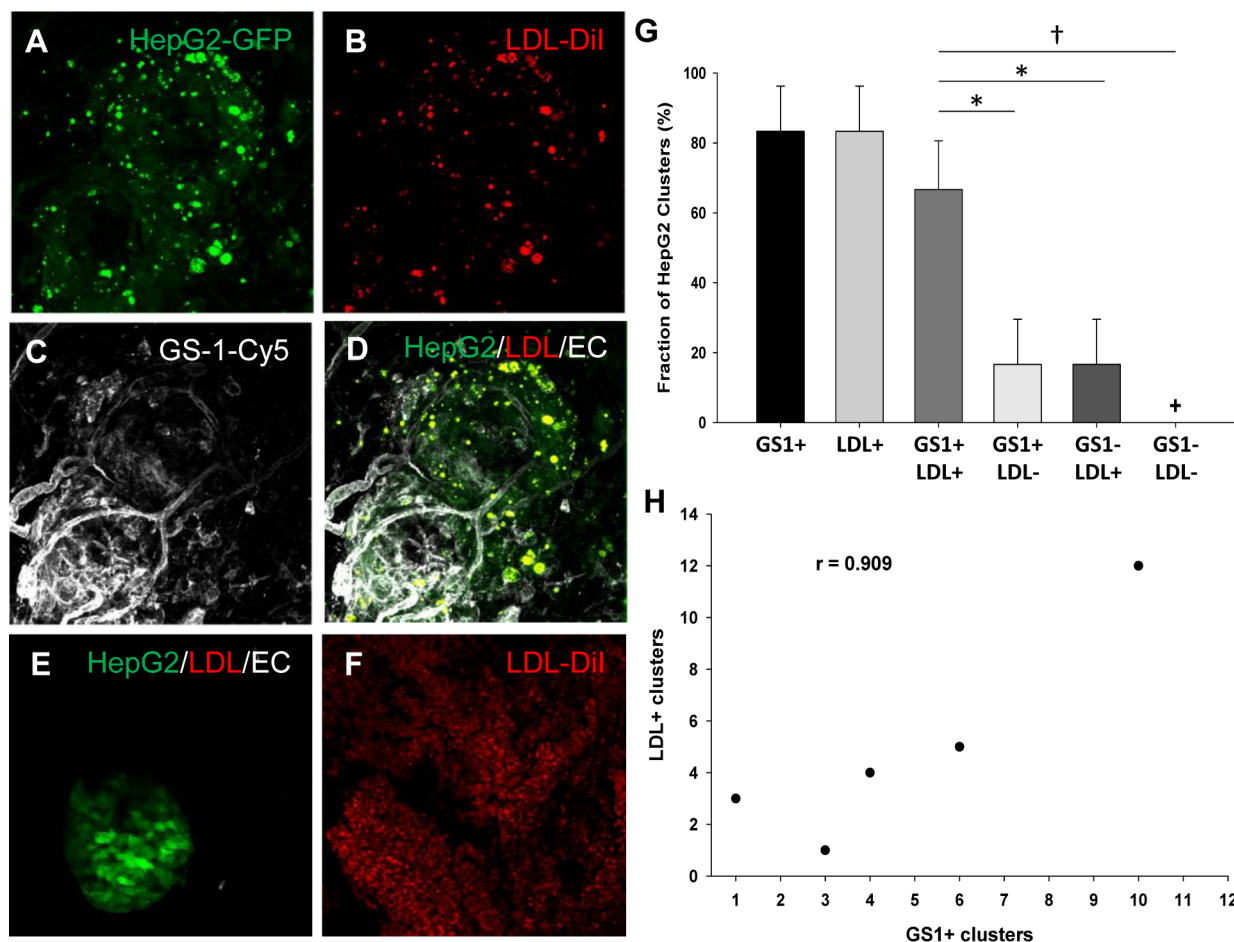


**Figure 5 |** Freshly isolated adipose SVF cells form a functional interface with implanted parenchymal cells that allows for DiI-LDL uptake. (A) HepG2-GFP<sup>+</sup> coated Cytodex-3 microcarrier beads. (B) DiI-LDL within construct. (C) GS1-Cy5<sup>+</sup> staining of murine endothelium, demonstrating formation of a vascular bed around beads. (D) HepG2-GFP<sup>+</sup> and DiI-LDL overlay showing co-localization. (E) HepG2-GFP<sup>+</sup> coated Cytodex-3 microcarrier beads implanted without SVF cells do not form a GS1-Cy5<sup>+</sup> vascular network. No DiI-LDL uptake was observed. (F) DiI-LDL uptake within host liver confirming adequate DiI-LDL delivery to host circulation. (G) Percentage overlap of HepG2-GFP<sup>+</sup> clusters and GS1-Cy5<sup>+</sup> vasculature and DiI-LDL in implants containing SVFs and HepG2-GFP<sup>+</sup>. No HepG2 clusters lacking associated GS1-Cy5<sup>+</sup> and DiI-LDL signal were identified (+). \*p = 0.03; †p = 0.008 with n = 5/condition. At the 95% confidence level,  $\alpha = 0.569$ . Values are reported as mean  $\pm$  s.e.m. (H) Scatter plot of implants (n = 5/condition) with HepG2 clusters comparing DiI-LDL with GS1-Cy5<sup>+</sup> vasculature. Pearson correlation coefficient of r = 0.909 was calculated.

Although it is possible that vascular beds from all tissues<sup>22</sup>, when isolated and disassembled, would show the same self-assembly capacity as demonstrated here by adipose-derived SVF cells, the adipose vasculature has been proposed to be evolutionarily less mature than other more quiescent vascular beds and thus more plastic<sup>43</sup>. Perhaps this plasticity is important to allow tissue, and thus vascular, remodeling in response to the energy storage requirements of adipose tissue<sup>43</sup>. Besides its relative abundance and accessibility compared to other adult cell sources, these results highlight adipose-derived SVF clinical utility for vascularization under a variety of relevant conditions.

In conclusion, we demonstrate for the first time that adipose SVF cell-derived vasculatures from rodent and human sources can effectively integrate with host vessels and interface with parenchymal cells (model hepatocyte cells in this case) to form a functional, implanted tissue mimic module and proof-of-principle therapeutic potential. This enabling technology can also be expanded to generate a variety of tissue mimics and cellular modules, by simply changing the parenchymal cell type (e.g. cardiomyocytes,  $\beta$ -cells, or engineered therapeutic cells). The LDL uptake observation suggests that the adipose-derived vasculatures in these implant modules can acquire functional specificity, an important aspect for therapeutic efficacy and mimic function. This approach whereby abundant therapeutic

cells are utilized without selection or further manipulation, beyond the initial isolation process, creates new avenues towards tissue mimic and therapeutic applications including the ability to incorporate disease- and/or patient-specific dynamics.

## Methods

**Ethics statement.** All animal experiments were performed in compliance with institutional guidelines, as per US National Institutes of Health Guide for the Care and Use of Laboratory Animals and were approved by University of Louisville Institutional Animal Care and Use Committee procedures and policies (IACUC #12059, 12060).

**Rodent and human SVF isolation.** Adipose-derived SVF cells were isolated from the epididymal fat pads of male, retired breeder Sprague-Dawley rats (Charles River) under anesthesia [ketamine (40–80 mg/kg) and xylazine (5–10 mg/kg)]. Green fluorescent protein (GFP)-tagged SVF were obtained from Sprague-Dawley rats that ubiquitously express GFP (Rat Research and Resource Center, University of Missouri, Columbia, MO). Human SVF were isolated from adipose tissue obtained from abdominoplasty (IRB Exempt, #09.0037). Harvested fat was washed in 0.1% BSA-PBS, finely minced, and digested in 2 mg/ml type I collagenase solution (Worthington Biochemical Company, Freehold, NJ, USA) for 40 min at 37°C with vigorous shaking. Adipocytes were removed by centrifugation, and the entire cell pellet was washed with 0.1% BSA-PBS. Cells were either immediately used (Fresh SVF, fSVF) or plated into gelatin-coated plates (Cultured SVF, cSVF  $5 \times 10^4$  cells/cm<sup>2</sup>) in fresh media (DMEM supplemented with 2 mM L-glutamine, 50  $\mu$ g/ml ECGS and 10% FBS). Cultured SVF were used at P0 after 5–7 days when cells reached confluence.



**Flow cytometry analysis.** cSVF were dissociated with non-enzymatic Cell Dissociation Buffer (Sigma) after reaching confluence (P0) and fixed with 4% paraformaldehyde for 10 min at room temperature. Cells were blocked with PBS containing 5% fetal bovine serum (FBS) for 30 minutes on ice and incubated with the following antibodies in blocking buffer on ice for 1 hour: anti-CD14 (1 : 100), anti-CD31-APC (1 : 500) (BD Biosciences); anti-c-Kit (1 : 100, Abcam); anti-CXCR4 (1 : 100, Ebiosciences); anti-c-Met (1 : 100), anti-PDGFR- $\beta$  (1 : 100, Santa Cruz Biotechnology) overnight at 4 °C. Secondary antibodies used were anti-mouse-Alexa Fluor 488 (1 : 400) (Jackson ImmunoResearch) and anti-rabbit-Cy6 (1 : 500) (Jackson ImmunoResearch) for 30 min at 4 °C.

**Microvessel isolation.** Fat-derived microvessels (FMF) were isolated from rat epididymal fat by limited collagenase digestion and selective screening as previously described<sup>44,45</sup>. The collagenase used (type I; Worthington Biochemical Company, Freehold, NJ, USA) was lot tested to yield high numbers of fragments with intact morphologies. These vessel fragments have the potential to form a microcirculation composed of different vessel types 4 weeks post implantation in vivo in 3-dimensional collagen gels<sup>23</sup>.

**HepG2 cell culture.** HepG2 cells were cultured in T-75 tissue culture flasks in HepG2 growth media consisting of Dulbecco's Modified Eagle's Media high glucose, 10% fetal bovine serum, 1 × penicillin/streptomycin, and 1 × L-glutamine (Invitrogen Camarillo, CA, USA). Media was changed every other day and cells were grown to confluence at which time they were prepared for Cytodex-3 culture as described below. Plasmids and Cell Transduction HepG2 were transduced with retrovirus to constitutively express GFP (pBMN-I-GFP) or Ds-Red as previously described<sup>46</sup>.

**Cytodex-3 cell culture.** Fifty mg of Cytodex-3 microcarrier beads (Sigma, St. Louis, MO, USA) were hydrated with 5 mL phosphate buffered saline (PBS) -Ca<sup>2+</sup>/-Mg<sup>2+</sup> (Hyclone) for four hours with occasional mixing to avoid aggregation<sup>47,48</sup>. PBS solution was removed and washed out with freshly prepared 70% ethanol for total of four washes. The last 70% ethanol wash was carried overnight. The following day, ethanol was removed and 10 mL of HepG2 growth media was added for a total of four washes. The last wash was removed and HepG2 cells were passaged into a resuspension of 1 × 10<sup>6</sup> cells/mL. 6 × 10<sup>6</sup> cells were added to 4 mL of HepG2 media containing Cytodex-3 beads and gently mixed. The bead-cell mixture was added to a 100 mm petri dish (BD Falcon) and incubated for three days at 37 °C and 5% CO<sub>2</sub> for optimal microcarrier coverage.

**Preparation of 3-dimensional constructs and in vivo implantation.** To form the 3D constructs, fresh or cultured SVF (10<sup>6</sup> cells/mL) were suspended into 3 mg/mL of collagen type I (BD Biosciences, San Jose, CA, USA) and 0.2 mL of the suspension was seeded into wells of 48-well culture plates. Constructs were implanted subcutaneously on the flanks of Rag1 mice as previously described<sup>22</sup>. To assess the potential of fresh and cultured SVF to participate in the neovascularization process, fresh or cultured SVF from GFP rats (10<sup>6</sup> cells/mL) were seeded into collagen gels concomitantly with isolated FMFs (20,000/mL). FMF/SVF/collagen suspensions were pipetted into wells of a 48-well culture plate (0.2 mL/well) to form a 3D construct that were either cultured in DMEM + 10% FBS or implanted subcutaneously on the flanks of Rag1 mice as previously<sup>24</sup>. Alternatively, SVF were seeded in the presence of HepG2 cells before implantation.

**Implant analysis.** Microvascular constructs were harvested at either 4 or 6 weeks after implantation and fixed in 4% paraformaldehyde for 20 minutes. Samples were permeabilized with 0.5% Triton X-100 and rinsed with PBS. After blocking for two hours with 10% goat serum (Sigma), samples were incubated overnight with fluorescent or biotin conjugated lectins. Following three 15 minute washes in divalent cation free (DCF)-PBS, samples were imaged en bloc with an Olympus MPE FV1000 Confocal Microscope and analyzed with Amira 5.2 (Visage Imaging, Inc., San Diego, CA, USA). SVF cells were identified by either constitutive expression of GFP (when obtained from animals that ubiquitously and constitutively express GFP) or labeling with TRITC/Fluorescence conjugated or Cy5-streptavidin GSI (rodent SVF) or UEAI (human SVF) lectin (Vector labs, Burlingame, CA, USA). To evaluate vessel perfusion in the implanted constructs, host mice were perfused intravenously with the blood tracer dextran-TRITC 2,000,000 MW for 15 minutes before the constructs were harvested. Confocal microscopy images of implants (from 3–12 image stacks per each of 5 implants) with HepG2-GFP<sup>+</sup> clusters were identified and examined for presence of GS1-Cy5<sup>+</sup> vasculature, DiI-LDL, or both. Those images without HepG2-GFP<sup>+</sup> clusters were not included. Significant differences between HepG2-GFP<sup>+</sup> clusters with both GS1-Cy5<sup>+</sup> vessels and DiI-LDL and those with either one or the other or none were determined using a two-tailed t-test between the sample pairs of interest. To determine if DiI-LDL uptake is correlated with the presence of GS1-Cy5<sup>+</sup> vasculature, HepG2-GFP<sup>+</sup> clusters positive for DiI-LDL were plotted against those clusters positive for GS1-Cy5<sup>+</sup> vasculature. The Pearson correlation coefficient was then calculated for statistical correlation between the two variables. Significant differences in measured parameters (Figs. 1–3) between fresh and cultured SVF cells (n = 3/condition) was determined by a Student's t-test with a normality check.

1. Fox, I. J. & Roy-Chowdhury, J. Hepatocyte transplantation. *J. Hepatol.* **40**, 878–886 (2004).

2. Strom, S. C. *et al.* Transplantation of human hepatocytes. *Transplant. Proc.* **29**, 2103–2106 (1997).
3. Habibullah, C. M., Syed, I. H., Qamar, A. & Taher-Uz, Z. Human fetal hepatocyte transplantation in patients with fulminant hepatic failure. *Transplantation* **58**, 951–952 (1994).
4. Nagata, H. *et al.* Prolonged survival of porcine hepatocytes in cynomolgus monkeys. *Gastroenterology* **132**, 321–329 (2007).
5. Kaully, T., Kaufman-Francis, K., Lesman, A. & Levenberg, S. Vascularization--the conduit to viable engineered tissues. *Tissue Eng. Part B Rev.* **15**, 159–169 (2009).
6. Chiu, L. L., Iyer, R. K., Reis, L. A., Nunes, S. S. & Radisic, M. Cardiac tissue engineering: current state and perspectives. *Front. Biosci.* **17**, 1533–1550 (2012).
7. Jain, R. K. Molecular regulation of vessel maturation. *Nat. Med.* **9**, 685–693 (2003).
8. Markkanen, J. E., Rissanen, T. T., Kivela, A. & Yla-Herttuala, S. Growth factor-induced therapeutic angiogenesis and arteriogenesis in the heart--gene therapy. *Cardiovasc. Res.* **65**, 656–664 (2005).
9. Gimble, J. M., Katz, A. J. & Bunnell, B. A. Adipose-derived stem cells for regenerative medicine. *Circ. Res.* **100**, 1249–1260 (2007).
10. Gimble, J. M., Bunnell, B. A., Chiu, E. S. & Guilak, F. Concise review: Adipose-derived stromal vascular fraction cells and stem cells: let's not get lost in translation. *Stem Cells* **29**, 749–754 (2011).
11. Han, J. *et al.* Adipose tissue is an extramedullary reservoir for functional hematopoietic stem and progenitor cells. *Blood* **115**, 957–964 (2010).
12. Yoshimura, K. *et al.* Characterization of freshly isolated and cultured cells derived from the fatty and fluid portions of liposuction aspirates. *J. Cell. Physiol.* **208**, 64–76 (2006).
13. Rehman, J. *et al.* Secretion of angiogenic and antiapoptotic factors by human adipose stromal cells. *Circulation* **109**, 1292–1298 (2004).
14. Koh, Y. J. *et al.* Stromal vascular fraction from adipose tissue forms profound vascular network through the dynamic reassembly of blood endothelial cells. *Arterioscler. Thromb. Vasc. Biol.* **31**, 1141–1150 (2011).
15. Cervelli, V. *et al.* Application of enhanced stromal vascular fraction and fat grafting mixed with PRP in post-traumatic lower extremity ulcers. *Stem Cell Res.* **6**, 103–111 (2011).
16. Premaratne, G. U. *et al.* Stromal vascular fraction transplantation as an alternative therapy for ischemic heart failure: anti-inflammatory role. *J. Cardiothorac. Surg.* **6**, 43 (2011).
17. Leblanc, A. J., Touroo, J. S., Hoying, J. B. & Williams, S. K. Adipose stromal vascular fraction cell construct sustains coronary microvascular function after acute myocardial infarction. *Am. J. Physiol. Heart Circ. Physiol.* **302**, H973–982 (2012).
18. Williams, S. K., Wang, T. F., Castrillo, R. & Jarrell, B. E. Liposuction-derived human fat used for vascular graft sodding contains endothelial cells and not mesothelial cells as the major cell type. *J. Vasc. Surg.* **19**, 916–923 (1994).
19. Cardinal, K. O., Bonnema, G. T., Hofer, H., Barton, J. K. & Williams, S. K. Tissue-engineered vascular grafts as in vitro blood vessel mimics for the evaluation of endothelialization of intravascular devices. *Tissue Eng.* **12**, 3431–3438 (2006).
20. Traktuev, D. O. *et al.* A population of multipotent CD34-positive adipose stromal cells share pericyte and mesenchymal surface markers, reside in a periendothelial location, and stabilize endothelial networks. *Circ. Res.* **102**, 77–85 (2008).
21. Lois, C., Hong, E. J., Pease, S., Brown, E. J. & Baltimore, D. Germline transmission and tissue-specific expression of transgenes delivered by lentiviral vectors. *Science* **295**, 868–872 (2002).
22. Nunes, S. S. *et al.* Angiogenic potential of microvessel fragments is independent of the tissue of origin and can be influenced by the cellular composition of the implants. *Microcirculation* **17**, 557–567 (2010).
23. Nunes, S. S., Rekapally, H., Chang, C. C. & Hoying, J. B. Vessel arterial-venous plasticity in adult neovascularization. *PLoS One* **6**, e27332 (2011).
24. Nunes, S. S. *et al.* Implanted microvessels progress through distinct neovascularization phenotypes. *Microvasc. Res.* **79**, 10–20 (2009).
25. Knowles, B. B., Howe, C. C. & Aden, D. P. Human hepatocellular carcinoma cell lines secrete the major plasma proteins and hepatitis B surface antigen. *Science* **209**, 497–499 (1980).
26. Agius, L., Battersby, C. & Alberti, K. G. Monolayer culture of parenchymal rat hepatocytes on collagen-coated microcarriers. A hepatocyte system for short- and long-term metabolic studies. *In Vitro Cell. Dev. Biol.* **21**, 254–259 (1985).
27. Pak, Y. K. *et al.* Activation of LDL receptor gene expression in HepG2 cells by hepatocyte growth factor. *J. Lipid Res.* **37**, 985–998 (1996).
28. Pinheiro, C. H. *et al.* Local injections of adipose-derived mesenchymal stem cells modulate inflammation and increase angiogenesis ameliorating the dystrophic phenotype in dystrophin-deficient skeletal muscle. *Stem Cell Rev.* **8**, 363–374 (2012).
29. Takahashi, K. *et al.* Induction of pluripotent stem cells from adult human fibroblasts by defined factors. *Cell* **131**, 861–872 (2007).
30. Cai, J. *et al.* Directed differentiation of human embryonic stem cells into functional hepatic cells. *Hepatology* **45**, 1229–1239 (2007).
31. Mizuno, H., Tobita, M. & Uysal, A. C. Concise review: Adipose-derived stem cells as a novel tool for future regenerative medicine. *Stem Cells* **30**, 804–810 (2012).
32. Kedem, A. *et al.* Vascular endothelial growth factor-releasing scaffolds enhance vascularization and engraftment of hepatocytes transplanted on liver lobes. *Tissue Eng.* **11**, 715–722 (2005).



33. Broudy, V. C. *et al.* Human umbilical vein endothelial cells display high-affinity c-kit receptors and produce a soluble form of the c-kit receptor. *Blood* **83**, 2145–2152 (1994).
34. Lammie, A. *et al.* Expression of c-kit and kit ligand proteins in normal human tissues. *J. Histochem. Cytochem.* **42**, 1417–1425 (1994).
35. Majumder, S., Brown, K., Qiu, F. H. & Besmer, P. c-kit protein, a transmembrane kinase: identification in tissues and characterization. *Mol. Cell. Biol.* **8**, 4896–4903 (1988).
36. Abramsson, A., Lindblom, P. & Betsholtz, C. Endothelial and nonendothelial sources of PDGF-B regulate pericyte recruitment and influence vascular pattern formation in tumors. *J. Clin. Invest.* **112**, 1142–1151 (2003).
37. Bjarnegard, M. *et al.* Endothelium-specific ablation of PDGFB leads to pericyte loss and glomerular, cardiac and placental abnormalities. *Development* **131**, 1847–1857 (2004).
38. Zhao, Y., Waldman, S. D. & Flynn, L. E. Multilineage co-culture of adipose-derived stem cells for tissue engineering. *J. Tissue Eng. Regen. Med.* (2012).
39. Boyd, N. L. *et al.* Dissecting the role of human embryonic stem cell-derived mesenchymal cells in human umbilical vein endothelial cell network stabilization in three-dimensional environments. *Tissue Eng. Part A* **19**, 211–223 (2013).
40. Koike, N. *et al.* Tissue engineering: creation of long-lasting blood vessels. *Nature* **428**, 138–139 (2004).
41. Stratman, A. N., Malotte, K. M., Mahan, R. D., Davis, M. J. & Davis, G. E. Pericyte recruitment during vasculogenic tube assembly stimulates endothelial basement membrane matrix formation. *Blood* **114**, 5091–5101 (2009).
42. Eto, H. *et al.* Characterization of Human Adipose Tissue-Resident Hematopoietic Cell Populations Reveals a Novel Macrophage Subpopulation with CD34 Expression and Mesenchymal Multipotency. *Stem Cells Dev.* **22**, 985–997 (2013).
43. Rupnick, M. A. *et al.* Adipose tissue mass can be regulated through the vasculature. *Proc. Natl. Acad. Sci. U. S. A.* **99**, 10730–10735 (2002).
44. Chang, C. C. *et al.* Angiogenesis in a microvascular construct for transplantation depends on the method of chamber circulation. *Tissue Eng. Part A* **16**, 795–805 (2010).
45. Hoying, J. B., Boswell, C. A. & Williams, S. K. Angiogenic potential of microvessel fragments established in three-dimensional collagen gels. *In Vitro Cell. Dev. Biol. Anim.* **32**, 409–419 (1996).
46. Boyd, N. L. *et al.* Microvascular mural cell functionality of human embryonic stem cell-derived mesenchymal cells. *Tissue Eng. Part A* **17**, 1537–1548 (2011).
47. Carmona, R. *et al.* Immunolocalization of the transcription factor Slug in the developing avian heart. *Anat. Embryol. (Berl)* **201**, 103–109 (2000).
48. Gao, Y., Hu, H. Z., Chen, K. & Yang, J. Z. Primary porcine hepatocytes with portal vein serum cultured on microcarriers or in spheroidal aggregates. *World Journal of Gastroenterology* **6**, 365–370 (2000).

## Acknowledgments

Authors would like to thank Kaitlin Shumate for technical assistance.

## Author contributions

Experimental Design and Interpretation: S.S.N., J.G.M., L.K., V.M.R., S.K.W., J.B.H., N.L.B.; Data acquisition and data analysis: S.S.N., J.G.M., L.K., V.M.R., L.R.C., J.B.H., N.L.B.; Draft/revise manuscript: S.S.N., J.G.M., J.B.H., N.L.B.; In vivo models: S.S.N., J.G.M., V.M.R.; Microscopy: S.S.N., J.G.M., V.M.R.; Cytometry: S.S.N., L.R.C.; Image processing and statistical analysis: S.S.N., J.G.M., L.K.; Administrative and technical support: S.K.W., J.B.H., N.L.B., S.S.N., J.B.H. and N.L.B. wrote the main manuscript text. S.S.N. contributed to figures 1–4. J.G.M. and V.M.R. contributed with figures 4–5. L.K. contributed to figure 2. L.R.C. contributed to figure 3. S.K.W., J.G.H. and N.L.B. provided administrative and technical support. All authors reviewed the manuscript.

## Additional information

**Funding:** N.L.B.: AHA 11SDG7500025 and Kosair Children’s Charity Development Grant; J.B.H.: EB007556 and P30GM103507; S.K.W.: DK078175; and the Gheens Foundation, Inc.

**Competing financial interests:** The authors declare no competing financial interests.

**How to cite this article:** Nunes, S.S. *et al.* Generation of a functional liver tissue mimic using adipose stromal vascular fraction cell-derived vasculatures. *Sci. Rep.* **3**, 2141; DOI:10.1038/srep02141 (2013).



This work is licensed under a Creative Commons Attribution-NonCommercial-ShareAlike 3.0 Unported license. To view a copy of this license, visit <http://creativecommons.org/licenses/by-nc-sa/3.0>